

# 38-krad/s 3.8-Grad Broadband Endless Optical Polarization Tracking Using LiNbO<sub>3</sub> Device

Reinhold Noé, *Member, IEEE*, Benjamin Koch, *Student Member, IEEE*, Vitali Mirvoda, Ariya Hidayat, and David Sandel, *Member, IEEE*

**Abstract**—We demonstrate automatic endless optical polarization tracking over 3.8 Grad at up to 38-krad/s control speed with mean/maximum polarization errors of 0.068/0.185 rad. Without polarization fluctuations, mean/maximum polarization errors are 0.05/0.1 rad. Small-signal control time constant is about 2  $\mu$ s. Function is maintained over the wavelength range 1505–1570 nm.

**Index Terms**—Optical fiber communication, optical fiber polarization, quadrature phase-shift keying (PSK).

## I. INTRODUCTION

**P**OLARIZATION-MULTI-MULTEPLEXED (PDM) transmission systems with direct detection avoid the high-speed, high-power electronics required for coherent polarization-diversity detection at high bitrates. On the other hand, optical polarization demultiplexing requires automatic polarization control [1]–[4], which should be fast and endless: In the field [5], significant polarization changes have been observed within periods of about 100  $\mu$ s. Much faster changes are possible if a dispersion-compensating fiber reel is hit hard. Endless means that the instantaneous polarization mismatch is bounded and small at all times, even if the tracked polarization moves around the Poincaré sphere many or an unlimited number of times. Short glitches would already cause a large number of bit errors that could not be corrected by forward error correction.

Starting from  $\sim$ 0.1 rad/s achieved in 1987 [6], the past two decades have brought the maximum endless polarization tracking speed to 15 krad/s [7]. Averaged over this long period, speed has doubled approximately every 14 months. Other authors have reported a 4.9-krad/s speed [8] with ten periods of one particular repetitive endless Poincaré sphere trajectory tracked in 20 ms. A 12.6-krad/s speed was given in [9] while tracking seemingly finite rather than endless polarization changes. To the best of our knowledge, more high-speed optical polarization control experiments have not been reported by other authors.

Manuscript received April 26, 2009; revised May 18, 2009. First published August 07, 2009; current version published August 19, 2009. This work was supported in part by Deutsche Forschungsgemeinschaft.

R. Noé, B. Koch, V. Mirvoda, and D. Sandel are with the University of Paderborn, 33098 Paderborn, Germany (e-mail: noe@upb.de; koch@ont.upb.de).

A. Hidayat was with the University of Paderborn, 33098 Paderborn, Germany. He is now with Nokia, Qt Software, 0402 Oslo, Norway.

Color versions of one or more of the figures in this letter are available online at <http://ieeexplore.ieee.org>.

Digital Object Identifier 10.1109/LPT.2009.2024549

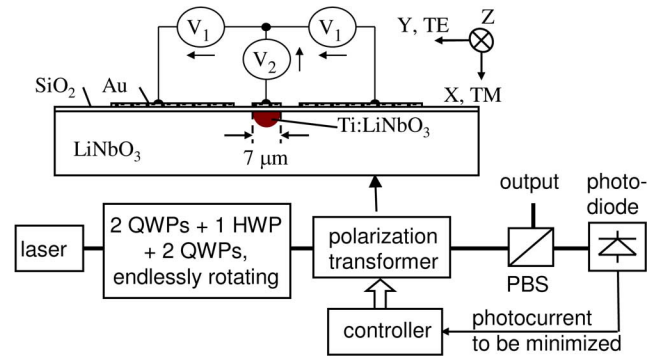


Fig. 1. Setup for endless polarization control with integrated-optical LiNbO<sub>3</sub> component containing eight electrooptic wave plates.

We have recently tracked endless polarization changes:

- Step 1) In a 112-Gb/s PDM differential quadrature phase-shift keying (DQPSK) field trial at 800-rad/s speed [1];
- Step 2) In a setup like Fig. 1, from 0 °C to 70 °C, from 1520 to 1564 nm, and on a 2.5-Grad-long trajectory, all at 14-krad/s speed [10].

As will be seen, the latter speed is not the limit.

## II. ENDLESS POLARIZATION CONTROL SETUP

Endless optical polarization control requires at least one Soleil–Babinet compensator (SBC), i.e., a rotary linear wave plate with adjustable retardation [6], [7], [10]. In our control system (see Fig. 1), a commercial polarization transformer (EOSPACE) contains a cascade of eight such integrated-optical wave plates implemented in X-cut, Z-propagation LiNbO<sub>3</sub>. Voltage  $V_1$  shifts the TE versus TM phase difference, while voltage  $V_2$  converts TE into TM and *vice versa*. Both voltages allow to realize a retarder with adjustable retardation and linear eigenmodes.

In the experimental setup, the controller is used to stabilize the polarization-scrambled signal of an unmodulated laser source. The output signal of the polarization controller is fed into a polarization beam splitter (PBS). One of its output signals is detected and used for feedback to the controller. By modulating the control voltages, a gradient algorithm, implemented in a field-programmable gate array (FPGA), seeks and reaches a global intensity minimum. As a consequence, the other PBS output provides full intensity.

We found that controlling more than one wave plate simultaneously by the gradient algorithm reduces required voltages, and greatly increases tolerance against device-inherent nonideal

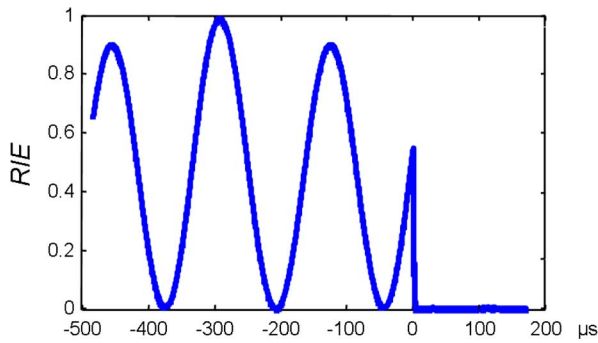


Fig. 2. Relative intensity error (RIE) versus time for 38-krad/s trajectory with controller switched on at  $t = 0 \mu\text{s}$ .

behavior and variations of the fixed output polarization. The reachable control speed is, therefore, improved.

### III. EXPERIMENTAL RESULTS

To achieve highest scrambling speeds, a fast rotary half-wave plate (HWP) is placed between two pairs of fiber-optic quarter-wave plates (QWP), which rotate endlessly at unequal rates of 0.88, 5.2, 5.68, and  $-0.96$  Hz. The HWP is realized by an additional LiNbO<sub>3</sub> polarization transformer that endlessly rotates the eigenmodes of the SBCs at a constant retardation of  $\pi$ . With linear polarization at the input, one HWP voltage period will generate  $4\pi$  polarization rotation at the output. At a drive frequency of 3.02 kHz, these polarization changes have a speed of 38 krad/s. Due to the two QWP pairs before and after the HWP, the output polarization mostly describes circles with different sizes and orientations. Mean (30 krad/s) and root-mean square scrambling speeds are  $\pi/4$  and  $\sqrt{2/3}$  times the maximum speed, respectively.

In Fig. 2, the QWPs are halted and aligned for linear HWP input polarization. This means that the HWP output polarization moves maximally fast, and passes through the points of minimum and maximum polarization error. The normalized feedback signal, i.e., the relative intensity error (RIE), is recorded in the FPGA, while the polarization controller is switched on at time  $t = 0 \mu\text{s}$ . In this case, it took  $\sim 5 \mu\text{s}$  for the controller to fully reach the global minimum.

From an analysis of another 100 switch-on processes from arbitrary polarizations but with initial errors  $< 1$  rad, we have assessed the small-signal control time constant to be on the order of  $2 \mu\text{s}$ . If signal acquisition from worst polarizations were problematic—which it is not—it could be speeded up by a systematic initial search.

To quantify control accuracy, the feedback signal, including the deviations caused by the voltage modulation, is recorded in the FPGA about every 229 ns, and put into a histogram. Fig. 3 shows the complementary distribution function  $1 - F$  (RIE) of the RIE, i.e., the probability that the RIE becomes worse than the value given on the abscissa. Results are shown for different scrambling speeds. Each curve stands for a measurement interval during  $\geq 5$  min. The leftmost trace shows a reference measurement without light to indicate measurement noise and determine the point of zero intensity error (RIE = 0). When the scrambler did not move (or was slow—there was not

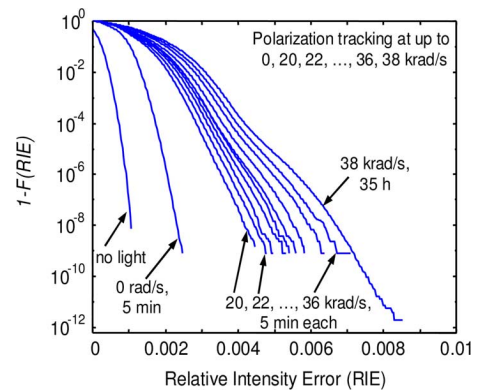


Fig. 3. Complementary distribution function  $1 - F$  (RIE) of RIE for different maximum polarization scrambling speeds.

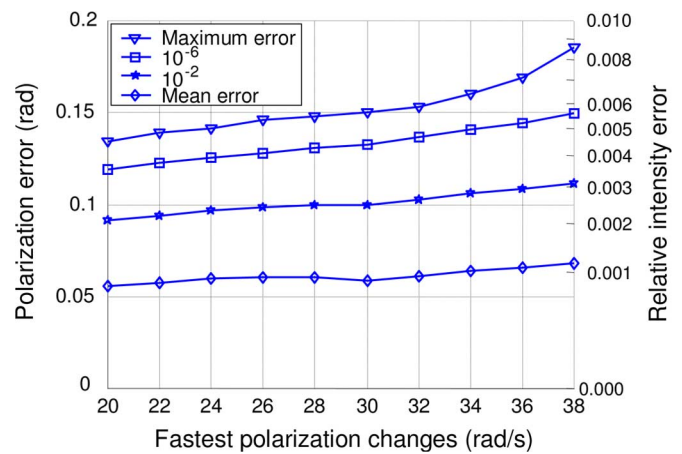


Fig. 4. RIE and polarization error that are surpassed only with the given probabilities, as a function of scrambling speed.

much difference), the mean/maximum RIE were 0.06%/0.25%. The mean/maximum polarization errors derived from this RIE are 0.05/0.1 rad. With the scrambler generating polarization changes up to 20 krad/s, mean/maximum RIE were measured to be 0.08%/0.45%, respectively. With maximally fast polarization changes of 38 krad/s, these errors were 0.11%/0.85%. The mean/maximum polarization errors corresponding to these are 0.068/0.185 rad. A more accurate value of the small-signal control time constant is, therefore, calculated as  $0.068 \text{ rad}/38 \text{ krad/s} = 1.8 \mu\text{s}$ . The 38-krad/s measurement was extended to a duration of 35 h to show long-term stability. Trajectory length during this last measurement is calculated as  $\sim 3.8$  Grad. Fig. 4 shows RIE and derived polarization error of the tracking experiments for various thresholds of the complementary distribution function. Since polarization-dependent outages typically last longer than a forward-error correction (FEC) frame, the bounded nature of the RIE that we measured is an indispensable asset.

The control behavior of the present polarization controller at 14-krad/s speed and room temperature is shown in Fig. 5. Overlaid with it are 15 traces of tests of our earlier polarization controller at 15 temperatures between  $0^\circ\text{C}$  and  $70^\circ\text{C}$  [10]. This tracking behavior is very reproducible, irrespective of temperature. Obviously, the earlier and the new polarization control

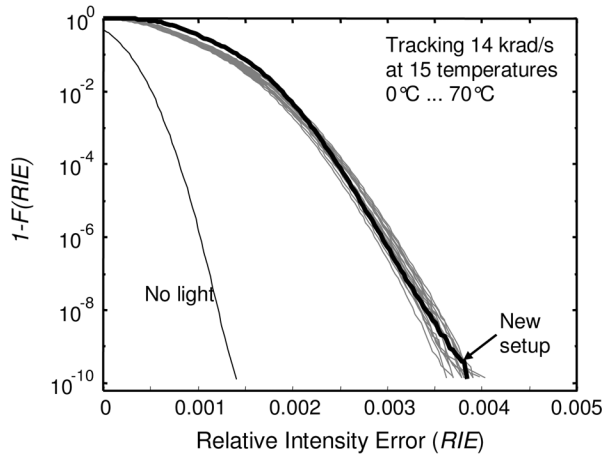


Fig. 5. Comparison of tracking experiments for 15 equispaced temperatures from 0 °C to 70 °C with old set up (gray traces) against measurement at room temperature with new set up (thick black trace). Each curve corresponds to 30 min.

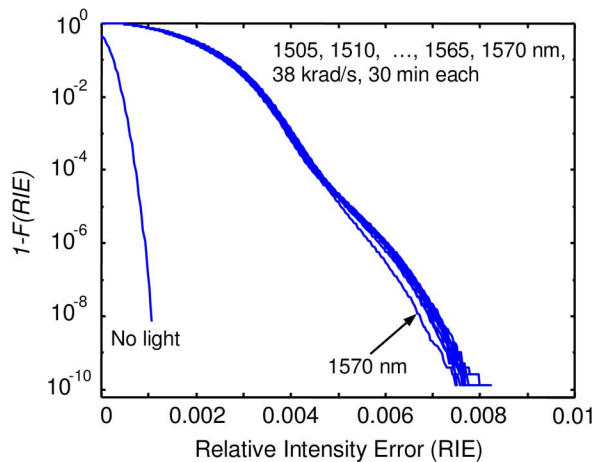


Fig. 6. Tracking up to 38 krad/s at 14 wavelengths 1505, 1510, ..., 1570 nm. At 1570 nm, there was slightly insufficient light power, which probably moved that trace to the left of the others.

system are of similar quality. A slight result discrepancy is still visible. It may be due to a  $>2$ -dB position-dependent loss of the bulk-optic HWP that was used in the old experiments instead of the electrooptic one. The position-dependent loss lets the intensity losses be underestimated.

The controller was also tested at 38-krad/s tracking speed for 14 equispaced wavelengths between 1505 and 1570 nm, 30 min each (see Fig. 6). Performance was again very uniform, benefiting from the presence of eight wave plates in the device. The 1570-nm trace seems to be a bit better than the others, but this is due to a slightly insufficient optical power at that wavelength, which in effect downscales the intensity.

#### IV. DISCUSSION AND CONCLUSION

Our polarization control speed is several to many times higher than that in [8] and [9], and tracked endless polarization trajectories are completely general and more than seven decades longer. Compared to [1], [7], and [10], several ingredients were changed: Since that controller is on loan for field trials [1], we built another unit with another LiNbO<sub>3</sub> device, suitable for higher tracking speed. Power consumption of the electrode voltage sources was halved to a total of  $\sim 5$  W. Tracking speed was increased from 14 (or 15) to 38 krad/s as follows: We improved the modulation scheme and simplified the basic control algorithm. And, we now use an electrooptic HWP in the scrambler with low position-dependent loss. Demonstrated wavelength tolerance range is now 65 nm instead of the earlier reported value of 44 nm.

With the aforescribed technology, 100 Gigabit Ethernet [(GbE) 28 Gbaud], or even  $2 \times 100$  GbE (56 Gbaud) PDM-DQPSK transponders can be developed today.

#### REFERENCES

- [1] H. Wernz, S. Bayer, B.-E. Olsson, M. Camera, H. Griesser, C. Fuerst, B. Koch, V. Mirvoda, A. Hidayat, and R. Noé, "112 Gb/s PolMux RZ-DQPSK with fast polarization tracking based on interference control," presented at the Proc. OFC/NFOEC 2009, San Diego, CA, Mar. 22–26, 2009, Paper OTuN4.
- [2] S. Bhandare, D. Sandel, B. Milivojevic, A. Hidayat, A. A. Fauzi, H. Zhang, S. K. Ibrahim, F. Wüst, and R. Noé, "5.94-Tb/s 1.49-b/s/Hz ( $40 \times 2 \times 2 \times 40$  Gb/s) RZ-DQPSK polarization-division multiplexed C-band transmission over 324 km," *IEEE Photon. Technol. Lett.*, vol. 17, no. 4, pp. 914–916, Apr. 2005.
- [3] M. Yagi, S. Satomi, and S. Ryu, "Field trial of 160-Gbit/s, polarization-division multiplexed RZ-DQPSK transmission system using automatic polarization control," presented at the Proc. OFC/NFOEC 2008, San Diego, CA, Feb. 24–28, 2008, Paper OThT7.
- [4] T. Ito, S. Fujita, E. T. de Gabory, and K. Fukuchi, "Improvement of PMD tolerance for 110 Gb/s pol-mux RZ-DQPSK signal with optical pol-dmux using optical PMD compensation and asymmetric symbol-synchronous chirp," presented at the Proc. OFC/NFOEC 2009, San Diego, CA, Mar. 22–26, 2009, Paper OThR5.
- [5] P. Krummrich, "Field trial results on statistics of fast polarization changes in long haul WDM transmission systems," presented at the Proc. OFC/NFOEC 2005, Anaheim, CA, Mar. 6–11, 2005, Paper OThT6.
- [6] R. Noé, H. Heidrich, and D. Hoffmann, "Endless polarization control systems for coherent optics," *J. Lightw. Technol.*, vol. 6, no. 7, pp. 1199–1208, Jul. 1988.
- [7] A. Hidayat, B. Koch, H. Zhang, V. Mirvoda, M. Lichtinger, D. Sandel, and R. Noé, "High-speed endless optical polarization stabilization using calibrated wave plates and field-programmable gate array-based digital controller," *Opt. Express*, vol. 16, no. 23, pp. 18984–18991, 2008.
- [8] F. Heismann and M. S. Whalen, "Fast automatic polarization control system," *IEEE Photon. Technol. Lett.*, vol. 4, no. 5, pp. 504–505, May 1992.
- [9] X. Zhang, G. Fang, X. Zhao, W. Zhang, L. Xi, Q. Xiong, and X. Li, "A novel endless polarization stabilizer with the additional function of stable SOP transformation in optical fiber communications," presented at the Proc. OFC/NFOEC 2009, San Diego, CA, Mar. 22–26, 2009, Paper JWA23.
- [10] B. Koch, A. Hidayat, V. Mirvoda, H. Zhang, D. Sandel, and R. Noé, "Robust, wavelength and temperature-insensitive 14 krad/s endless polarization tracking over 2.5 Grad," presented at the Proc. OFC/NFOEC 2009, San Diego, CA, Mar. 22–26, 2009, Paper JThA63.